

## Neutron Total Cross-Section Measurements and Resonance Parameter Analysis of Holmium, Thulium, and Erbium from 0.001 to 20 eV

Y. Danon,\* C. J. Werner, G. Youk,† R. C. Block, R. E. Slovacek, and N. C. Francis

*Rensselaer Polytechnic Institute, Environmental and Energy Engineering Department  
Troy, New York 12180-3590*

and

J. A. Burke, N. J. Drindak, F. Feiner, and J. A. Helm

*Lockheed Martin Corporation, P.O. Box 1072, Schenectady, New York 12301-1072*

*Received December 12, 1996*

*Accepted July 8, 1997*

**Abstract**—*The Rensselaer Polytechnic Institute linear accelerator with the enhanced thermal target was used for neutron transmission measurements of rare earth metal samples of holmium, erbium, and thulium and isotopically enriched oxide samples of  $^{166}\text{Er}_2\text{O}_3$  and  $^{167}\text{Er}_2\text{O}_3$  in the energy range from 0.001 to 20 eV. The measurements were done with a 15-m time-of-flight spectrometer and provided high-quality data in the thermal and subthermal region as well as in the low energy resonance region. The effect of paramagnetic scattering on these cross sections is discussed. The data were corrected for paramagnetic scattering, and resonance parameters were obtained by fitting the transmission with the SAMMY multilevel R-matrix code. These results were compared to the ENDF/B-VI evaluation and to other measurements.*

### I. INTRODUCTION

An enhanced thermal target (ETT) was recently installed at the Rensselaer Polytechnic Institute (RPI) linear accelerator<sup>1,2</sup> (LINAC). This target was designed to produce a high thermal flux required for thermal and subthermal cross-section measurements. The ETT provides a thermal neutron flux intensity that is approximately six times higher than that obtained with the previous “bounce target.”<sup>1</sup> The first measurements made with the ETT were a series of transmission measurements on the rare earth isotopes thulium, erbium, and holmium. As shown by Harris et al.<sup>3</sup> and Jonsson et al.,<sup>4</sup> precise knowledge of such capture cross sections allows accurate calculations of the

burnable poison effect and will reduce the error in  $k_{eff}$  in long-term burnup calculations.

The rare earth isotopes have a partially filled  $4f$  electron shell that causes a strong interaction between the atomic magnetic moment and the incident neutron magnetic moment, resulting in neutron paramagnetic scattering by the atom. This interaction is particularly strong in thulium, erbium, and holmium, whose paramagnetic scattering cross sections are in the range from 17 to 30 b at 0.0253 eV. This adds an additional complication to the analysis of the transmission measurements because the paramagnetic scattering reduces the measured transmission and requires a correction to determine the absorption cross section.

The raw data for each sample were reduced to transmission and corrected for paramagnetic scattering. Resonance parameters were then determined from the corrected transmission in the energy range from 0.001 to 20 eV.

\*Current address: Nuclear Research Center, Negev, P.O. Box 9001, Beer-Sheva, Israel.

†Current address: University of Florida, Gainesville, Florida.

TABLE I  
Metallic Erbium, Thulium, and Holmium Sample Thickness in Atoms per Barn\*

Erbium		Thulium		Holmium	
Nominal Thickness (cm)	Sample Thickness (atom/b)	Nominal Thickness (cm)	Sample Thickness (atom/b)	Nominal Thickness (cm)	Sample Thickness (atom/b)
0.0254	0.0008170 (0.10)	0.010	0.0003553 (0.05)	0.010	0.0003199 (0.05)
0.0508	0.0016672 (0.08)	0.025	0.0008522 (0.05)	0.030	0.0009459 (0.03)
0.127	0.0040916 (0.10)	0.100	0.0033136 (0.15)	0.100	0.0031763 (0.05)
0.254	0.0081558 (0.06)	0.2	0.0066484 (0.17)	0.3	0.0094784 (0.04)

\*The percent error is shown in parentheses.

## II. EXPERIMENTAL SETUP

The spectrometer is comprised of a 15-m flight path with the RPI LINAC and the ETT as the neutron source on one end and a 0.3-cm-thick lithium glass detector (6.6% lithium, enriched to 95% in  $^6\text{Li}$ ) at the other end of the flight path. The RPI LINAC was operated with an electron pulse width of 1  $\mu\text{s}$ , electron energy of 54 MeV, current on target of 8  $\mu\text{A}$ , and a repetition rate of 25 pulse/s. A 0.0127-cm-thick tungsten sample was inserted in the beam for all the erbium measurements to provide a blackout region near the 18.6-eV tungsten resonance, which was used for background normalization. A typical transmission experiment for several thicknesses of a given isotope took 30 h of data collection and an additional 6 h for background determination. The data were recorded on an HP-1000 (900 series) computer that also controlled the sample changer during the experiment. The sample changer can hold up to eight samples and rotate them in and out of the beam as controlled by the computer. Each run consisted of a cycle through all the samples with a predetermined number of LINAC pulses for each. The samples used were of different thicknesses and enrichment as shown in Tables I, II, and III. The oxide samples were prepared as a ceramic to reduce

the effect of  $\text{H}_2\text{O}$  that is usually present in the powder form. Normally, two of the sample positions were used to measure the open beam count rate and were placed at the beginning and middle of each sample cycle. The time split between the samples was optimized to reduce the counting statistics error in the transmission for a given run time.<sup>5</sup>

## III. DATA REDUCTION

The large amount of data collected in each of the experiments was first run through a statistical integrity check that verified the stability of the LINAC, the in-beam detector, and the beam monitors. This was done by checking the correlation between the counts from the monitors and the lithium glass in-beam detector and by tracking their correlation as a function of time. This check identified bad runs having counts lost from LINAC malfunctions and other problems in the system. The data were

TABLE II  
Ceramic Erbium Oxide Sample Thicknesses  
in Atoms per Barn\*

$^{166}\text{Er}_2\text{O}_3$	$^{167}\text{Er}_2\text{O}_3$	$\text{Er}_2\text{O}_3$
0.010263 (0.64)	0.006821 (0.59)	0.0034201 (0.03)

\*The percent error is shown in parentheses.

TABLE III  
Isotopic Composition of the Erbium Oxide  
Ceramic Samples

Isotope	$^{166}\text{Er}_2\text{O}_3$ Atom (%)	$^{167}\text{Er}_2\text{O}_3$ Atom (%)	$\text{Er}_2\text{O}_3$ Atom (%)
$^{162}\text{Er}$	0.00	0.00	0.14
$^{164}\text{Er}$	0.05	0.06	1.61
$^{166}\text{Er}$	96.24	2.93	33.6
$^{167}\text{Er}$	2.79	91.54	22.95
$^{168}\text{Er}$	0.75	5.14	26.8
$^{170}\text{Er}$	0.17	0.33	14.9
Total	100	100	100

then corrected for dead time, and runs were normalized and summed. Time-dependent background measurements were obtained with the one-notch, two-notch method.<sup>6</sup> The measured background was then fitted to a smooth analytical function of time of flight for each sample including the open beam measurement. The analytical expression was used for the background correction. Background is a first-order correction to the transmission. The magnitude of the correction depends on the signal-to-background ratio of the spectrometer. Typical open beam signal-to-background ratios at the RPI 15-m time-of-flight station with the ETT source vary between  $\sim 4000:1$  at 0.05 eV to  $\sim 8:1$  at 0.001 eV. Above 1 eV the signal-to-background ratio was  $\geq 50:1$ . Calculation of the transmission in time-of-flight channel  $i$  was obtained by

$$T_i = \frac{(C_i^s - K_s B_i - B_s)}{(C_i^o - K_o B_i - B_o)}, \quad (1)$$

where

$C_i^s, C_i^o$  = dead time corrected and normalized count rates of the sample and open measurements, respectively

$B_i$  = nominal time-dependent background count rate

$B_s, B_o$  = steady-state background counting rates for the sample and open measurements, respectively

$K_s, K_o$  = normalization factors for the sample and open measurements, respectively.

For erbium, the normalization factor  $K_o$  was determined by forcing the average transmission to zero in the blackout region of the strong 18.6-eV tungsten resonance. For the thulium and holmium samples, a black resonance in the sample was used. Similarly,  $K_s$  was calculated by forcing zero average transmission in the blackout region of strong resonances in the samples. The measured transmission from Eq. (1) was corrected for paramagnetic scattering before fitting the data to obtain resonance parameters.

#### IV. PARAMAGNETIC SCATTERING

Paramagnetic scattering contributes significantly to the thermal region ( $E_n < 0.1$  eV) total cross section of the rare earth metals. Paramagnetic scattering is a result of the interaction between the magnetic moment of the neutron and the target atom. The atom magnetic moment is due to interaction between the spin and orbital motion of the electron, where the nuclear contribution can be neglected. In the rare earth materials, the contribution to the atomic magnetic moment is mostly from the unfilled  $4f$  internal electron shell. The theory of neutron paramagnetic scattering from rare earth isotopes was given by Trammell<sup>7</sup> and later by Blume, Freeman, and Watson,<sup>8</sup>

who introduced a Hartree-Fock description for the free-ion many-electron problem. The total paramagnetic scattering is given by

$$\sigma_{pm} (\text{cm}^2) = \frac{2}{3} \pi \left( \frac{e^2}{mc^2} \right)^2 \gamma^2 \mu^2 f^2, \quad (2)$$

where

$f$  = form factor

$\gamma$  = neutron magnetic moment ( $1.9134\mu_N$ , taken from Ref. 9, and  $\mu_N$  is the nuclear magneton)

$\mu$  = atom magnetic moment ( $9.6\mu_B$  for erbium,  $10.6\mu_B$  for holmium, and  $7.6\mu_B$  for thulium, taken from Ref. 10, and  $\mu_B$  is the Bohr magneton)

$e^2/mc^2$  = classical radius of the electron ( $2.818 \times 10^{-13}$  cm).

The papers by Trammell<sup>7</sup> and Blume, Freeman, and Watson<sup>8</sup> show methods for obtaining the form factors as a function of the scattering angle and the neutron energy. Another calculation by Mattos<sup>11</sup> used the Hartree-Fock wave function and Blume's orbital and spin contribution functions to calculate the form factors. Mattos expanded the calculations to include the rare earths, holmium and thulium, which are of interest to this work. Mattos also averaged the squared form factors  $f^2$  over all scattering angles, which allows calculation of the energy-dependent paramagnetic cross section. A more accurate calculation was done by Stassis et al.,<sup>12</sup> which included relativistic effects of the electrons. The results of these calculations, as a function of neutron energy  $E$ , were fitted to an analytical function that is easier to use for the data correction. This function is in the form given by Trammell.<sup>7</sup> It yields an excellent fit and has only three parameters:  $A$ ,  $B$ , and  $p$ . When  $E$  is in electron volts,  $\sigma_{pm}$  is in barns,  $A$  is in (b)<sup>1/2</sup>, and  $B$  is in units of (eV)<sup>-p</sup>:

$$\sigma_{pm}(E) = \left\{ \frac{A}{BE^p} \frac{\tan^{-1}(BE^p)}{[1 + (BE^p)^2]^4} \right\}^2. \quad (3)$$

Equation (3) was fitted to the calculated Stassis paramagnetic cross section over the energy range  $0.001 \leq E \leq 0.1$  eV. Table IV shows the fitted parameters obtained.

Figure 1 shows the calculated paramagnetic scattering used for the transmission data correction. The calculation yields paramagnetic thermal (0.0253 eV) values of 15.7, 24.2, and 28.3 b for thulium, erbium, and holmium, respectively. The values calculated by Mattos are 17.3 b for thulium, 25.5 b for erbium, and 29.5 b for holmium. The relativistic calculation is  $\sim 5\%$  lower than the values calculated by Mattos. This difference is of the order of 1.4 b.

TABLE IV  
Parameters for the Fitted Paramagnetic Scattering  
Given in Eq. (3)

Isotope	$A$	$B$	$p$
Thulium	6.1691	1.1308	0.3367
Erbium	7.9012	1.1278	0.3263
Holmium	8.7597	1.1435	0.3225

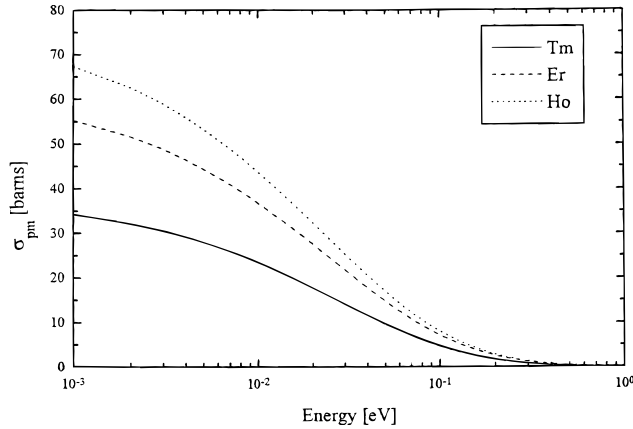


Fig. 1. Paramagnetic scattering cross sections calculated with Eq. (3).

## V. RESULTS

The transmissions of each of the holmium, erbium, thulium, and  $\text{Er}_2\text{O}_3$  samples were measured in separate experiments. To help display the thermal region data and compare them with other measurements, the data were first grouped into 512- $\mu\text{s}$  time-of-flight macrochannels, converted to cross section, and the cross sections were combined, weighted by their variances, to produce an average cross section at each energy bin. Only data points with transmission between 0.1 to 0.9 were included in the fit.

The resonance parameters for each isotope were obtained by fitting the transmission data with the multi-level  $R$ -matrix SAMMY code.<sup>13</sup> To use SAMMY, the transmission data were first corrected for paramagnetic scattering that SAMMY cannot handle. This correction was done by dividing the measured transmission by  $\exp(-N\sigma_{pm})$ , where  $N$  is the sample thickness and  $\sigma_{pm}$  is the paramagnetic cross section. The paramagnetic-scattering-corrected transmission data from all sample thicknesses were then fitted with SAMMY in a multiple sample fit procedure. The initial parameters for each fit were ENDF/B-VI parameters<sup>14</sup> except for the channel radii. For the channel radii, the values from Mughab-

ghab, Divadeenam, and Holden<sup>15</sup> were used. Negative resonance energies were not changed and only the neutron widths of negative energy resonances were fitted. The data were fitted starting with the thin sample; the covariance matrix and parameters calculated by SAMMY were then used for the next sample thickness, and so on. Because SAMMY is based on Bayesian analysis, the parameters and covariance matrix of the last calculation (normally the thickest sample) are the final results. Final runs were then made with the new parameters to generate the transmission for each sample thickness for comparison of measured and calculated transmission data.

A sensitivity analysis study of the importance of the thermal and subthermal data for the determination of the radiation widths in the lowest energy resonances indicates that these radiation widths can be determined from the thermal transmission data and are very sensitive to these data. This can be illustrated by using the simple single-level Breit-Wigner formula given by<sup>16</sup>

$$\sigma_t = \sigma_0 \left( \frac{E_0}{E} \right)^{1/2} \frac{\Gamma_n(\Gamma_n + \Gamma_\gamma)}{4(E - E_0)^2 + (\Gamma_n + \Gamma_\gamma)^2} \times \left[ 1 + \frac{4(E - E_0) R}{\Gamma_n + \Gamma_\gamma} \frac{R}{\lambda} \right] + \sigma_p \quad (4)$$

and calculating the transmission as

$$T(E) = e^{-N\sigma_t(E)}, \quad (5)$$

where  $N$  is the sample thickness.

The sensitivity of the transmission to the radiation width  $\Gamma_\gamma$  (which indicates the sensitivity of  $\Gamma_\gamma$  to changes in the cross section) is defined by

$$\text{sensitivity} = \frac{\left| \frac{\partial T(E)}{\partial \Gamma_\gamma} \right|}{T(E)}. \quad (6)$$

A plot of the sensitivity for the 0.46-eV resonance in  $^{167}\text{Er}$  is shown in Fig. 2 over the thermal energy region. The calculation was done for two different sample thicknesses (0.00508 and 0.0508 cm). The thermal cross section of the thicker sample was highly sensitive to the radiation width. Therefore, the data in the thermal region contain important information about the radiation width and were included in the fit region.

### V.A. Holmium

The total cross section (including paramagnetic scattering) in the thermal region is plotted in Fig. 3 together with several other measurements. The cross section is in good agreement with the measurement of Zimmerman et al.,<sup>17</sup> Schermer,<sup>18</sup> and Knorr and Schmatz.<sup>19</sup> In the energy region from 0.004 to 0.02 eV, the data follow the trend of the Schermer data and are higher than the measurement of Zimmerman et al.

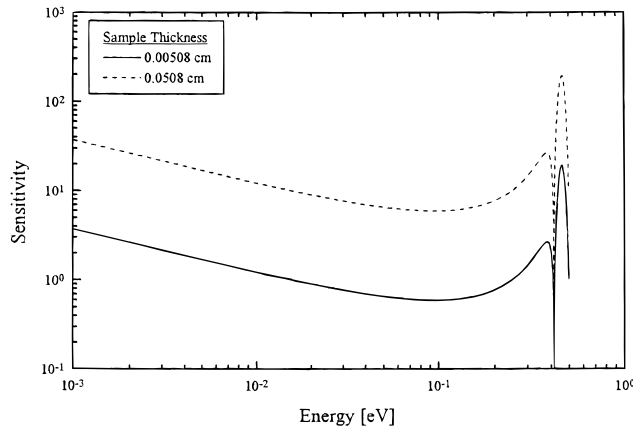


Fig. 2. The sensitivity of the transmission with respect to the gamma width of the 0.46-eV resonance in <sup>167</sup>Er. The sensitivity was calculated with Eq. (6) for two sample thicknesses. The transmission is more sensitive to the gamma width for the thicker sample.

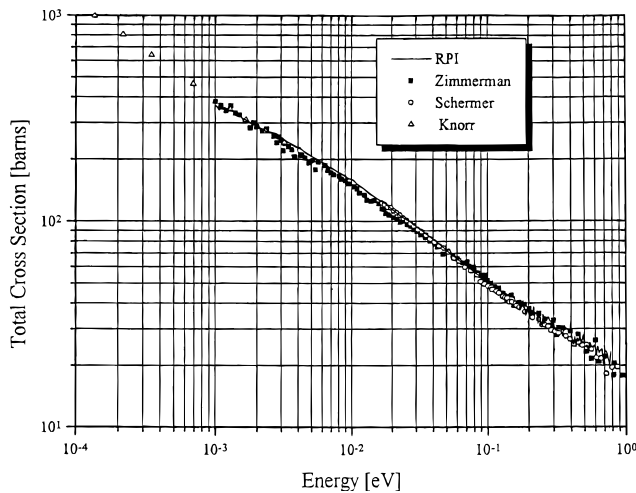


Fig. 3. Holmium thermal total cross section of the RPI data together with other experimental results.

Four sample thicknesses were used in the resonance parameter analysis; the results are listed in Table V together with parameters from Mughabghab, Divadeenam, and Watson<sup>15</sup> and ENDF/B-VI (Ref. 14). In comparing the neutron widths for the 8.16-eV holmium resonance from Mughabghab, ENDF/B-VI, and this measurement, the ENDF/B-VI value differs by a factor of 10; this, perhaps, is the result of a typographical error in the ENDF/B-VI value. The SAMMY fit is plotted in Fig. 4. The fitted data yielded a 0.0253-eV capture cross section of 64.4 b, which is in excellent agreement with the value of 64.7 b given in ENDF/B-VI. The errors listed for the parameters obtained in this measurement are the 1σ errors calculated by the SAMMY code.

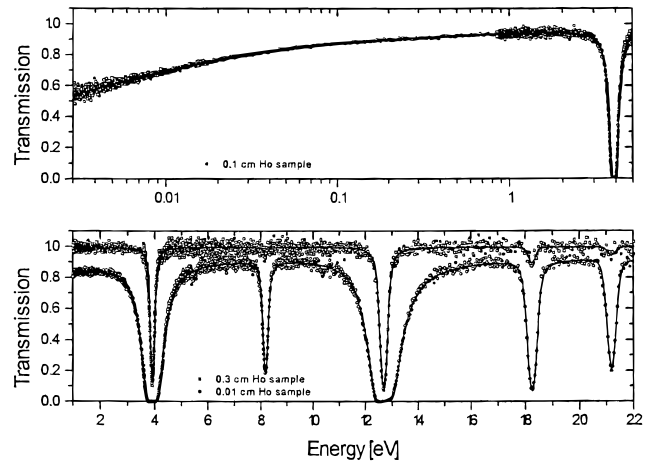


Fig. 4. Transmission data and SAMMY fit for holmium. Two sample thicknesses 0.01 and 0.3 cm are shown in the higher energy region. In the low-energy region, the fit is shown down to 0.003 eV.

### V.B. Erbium

Figure 5 shows the grouped thermal region cross section for the  $2.54 \times 10^{-3}$  cm sample together with other natural erbium measurements of Roesser and Slovacek,<sup>20</sup> Knorr and Schmatz,<sup>19</sup> and Zimmerman et al.<sup>17</sup> The measurement of Zimmerman et al. is in good agreement with the RPI measurement from 0.1 eV down to its lowest data point at 6 meV. The measurement of Roesser and Slovacek is ~12% lower in the region from 6 meV to 0.1 eV, and the cross-section slope of their measurement seems to be steeper. Knorr and Schmatz extended the cross-section

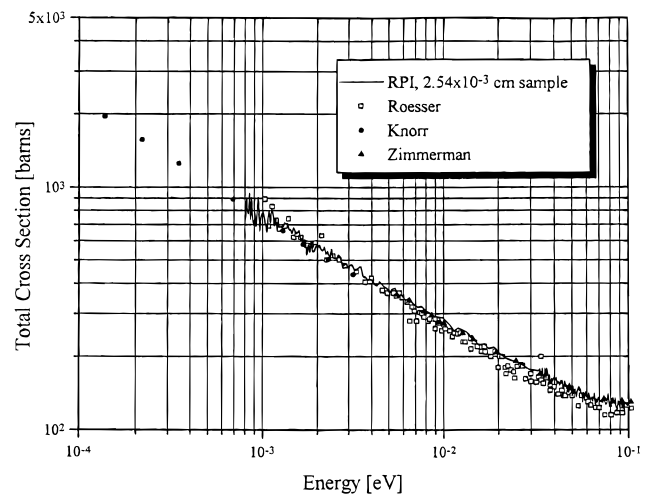


Fig. 5. Thermal cross section of natural erbium plotted with other measurements of Roesser and Slovacek,<sup>20</sup> Knorr and Schmatz,<sup>19</sup> and Zimmerman et al.<sup>17</sup>



TABLE V  
Summary of Fitted Resonance Parameters for Holmium\*

Mughabghab			ENDF/B-VI			RPI		
$E$ (eV)	$\Gamma_\gamma$ (meV)	$\Gamma_n$ (meV)	$E$ (eV)	$\Gamma_\gamma$ (meV)	$\Gamma_n$ (meV)	$E$ (eV)	$\Gamma_\gamma$ (meV)	$\Gamma_n$ (meV)
-10.9	77	62.108	---	---	---	-10.9	77	71.42 (0.53)
-6.31	77	14.089	---	---	---	-6.31	77	10.05 (0.12)
3.92 (0.01)	85 (2)	2.13 (0.09)	3.92	85	2.133	3.9141 (0.0001)	85.72 (0.29)	2.079 (0.0057)
8.16 (0.02)	89 (10)	0.187 (0.01)	8.16	78	1.874 <sup>a</sup>	8.1735 (0.0006)	94.15 (1.7)	0.1857 (0.0013)
10.32 (0.02)	---	0.027 (2g $\Gamma_n$ )						
12.75 (0.02)	---	10.489 (0.35)	12.75	78	10.49	12.690 (0.0004)	90.876 (0.88)	13.45 (0.09)
18.20 (0.02)	---	0.96 (0.06)	18.20	78	0.96	18.262 (0.0009)	78.055 (2.274)	1.255 (0.01)
21.12 (0.02)	84 (5)	0.56 (0.02)	21.12	78	0.56	21.194 (0.0016)	60.446 (3.5)	0.6522 (0.0071)

\*The errors are given in parentheses. The errors of the fitted parameters were calculated by SAMMY.

<sup>a</sup>This is probably a typographical error in ENDF/B-VI.

measurements down to  $\sim 0.15$  meV, and in the region from 1 to 3 meV they are  $\sim 7\%$  lower than the RPI measurement. However, the two experimental measurements agree within the experimental errors.

Six samples, including the erbium oxides, were used in the resonance parameter fit. The transmission of the oxide samples was corrected for the contribution from oxygen using a constant total cross section of 3.83 b (Ref. 5). The analysis of the  $^{167}\text{Er}_2\text{O}_3$  sample helped obtain better parameters for the 7.95-eV resonance in  $^{167}\text{Er}$ . In the natural erbium sample, this resonance has contributions from the 7.90-eV resonance in  $^{164}\text{Er}$ , and the two cannot be resolved. The fit is plotted in Fig. 6, and the fitted parameters are listed in Table VI. This erbium measurement resulted in a lower thermal capture cross section. The value of 155.1 b is  $\sim 4$  b lower than the value quoted by Mughabghab in Table VII. Also, the thermal capture cross sections of  $^{166}\text{Er}$  and  $^{167}\text{Er}$  are lower than the value quoted by Mughabghab.

### V.C. Thulium

The cross sections are plotted in Fig. 7 with the measurements of Knorr and Schmatz<sup>19</sup> and Zimmerman et al.<sup>17</sup> Below 0.04 eV, the data are in excellent agreement with the measurement of Zimmerman et al.; how-

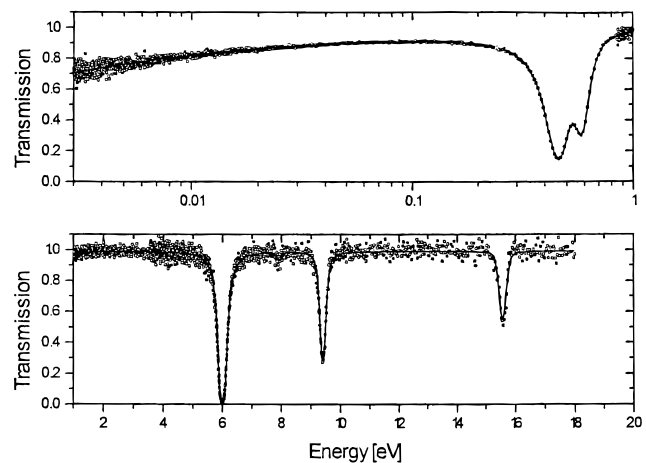


Fig. 6. Transmission data and SAMMY fit for the 0.0254-cm-thick erbium sample. A total of six samples were used including enriched  $^{166}\text{Er}$  and  $^{167}\text{Er}$ .

ever, above 0.04 eV, the RPI data are slightly lower. The SAMMY fit results are plotted in Fig. 8, and the fitted resonance parameters are listed in Table VIII. Also shown in Table VIII are Mughabghab's parameters for thulium. Note that no ENDF/B-VI values were available.

TABLE VI  
Erbium Resonance Parameters\*

Mughabghab			ENDF/B-VI			RPI		
$E$ (eV)	$\Gamma_\gamma$ (meV)	$\Gamma_n$ (meV)	$E$ (eV)	$\Gamma_\gamma$ (meV)	$\Gamma_n$ (meV)	$E$ (eV)	$\Gamma_\gamma$ (meV)	$\Gamma_n$ (meV)
-40.4	92	482.4	-40.4	92	488.7	-40.4	92	395.3 (0.3)
0.46 (0.02)	88 (1.0)	0.279 (0.004)	0.46	88	0.2791	0.4595 (0.0001)	87.12 (0.16)	0.2694 (0.0006)
0.584 (0.002)	86.3 (1.0)	0.256 (0.005)	0.584	86.3	0.2560	0.5834 (0.0002)	86.20 (0.33)	0.2472 (0.0009)
5.98 (0.02)	84 (4)	20.2 (1.1)	5.98	84	20.23	5.9936 (0.0006)	104.9 (2.1)	20.71 (0.30)
7.90 (0.02)	96	0.65 (0.08)				7.90	96	0.71 (0.03)
7.95 (0.03)	---	0.196 (0.018)	7.95	89	0.1956	7.93 (0.002)	98.82 (4.5)	0.160 (0.005)
9.37 (0.05)	84 (9)	8.0 (0.5)	9.37	84	8.0	9.389 (0.001)	88.3 (2.0)	9.20 (0.14)
15.55 (0.04)	94 (6)	2.2 (0.15)	15.55	94	2.2	15.567 (0.003)	76.8 (4.1)	2.63 (0.10)

\*Errors are in parentheses.

TABLE VII  
Thermal Capture and Total Cross Sections for Thulium, Erbium, and Holmium

	Capture Cross Section (b)			Total Cross Section (b)		
	Mughabghab, Divadeenam, and Watson	ENDF/B-VI	RPI <sup>a</sup>	Mughabghab, Divadeenam, and Watson	ENDF/B-VI <sup>b</sup>	RPI
Thulium	105 ± 2	Not in ENDF/B-VI	109.0 ± 0.7 ± 1.6	134.3 ± 3.6	Not in ENDF/B-VI	133.3 ± 0.9
Erbium	159.2 ± 3.6	Not in ENDF/B-VI	155.1 ± 1.2 ± 2.4	194.3 ± 4.4	Not in ENDF/B-VI	189.5 ± 1.5
<sup>166</sup> Er	19.6 ± 1.5	19.6	16.2 ± 0.2 ± 2.4	59.9 ± 3.6	35.5	53.8 ± 0.6
<sup>167</sup> Er	659 ± 16	657.8	644.4 ± 3.3 ± 2.4	686.7 ± 16.2	662.7	675.6 ± 3.5
Holmium	64.7 ± 1.2	64.7	64.4 ± 0.3 ± 2.8	98.0 ± 2.7	74.2	102.5 ± 0.5

<sup>a</sup>The first set of errors is based on the statistical accuracy of the total cross-section measurement, and the second set of errors is our estimated uncertainty in the paramagnetic and nuclear scattering subtraction.

<sup>b</sup>The ENDF/B-VI total cross section does not include paramagnetic scattering.

#### V.D. Summary of Thermal Results

The total and capture thermal cross sections are listed in Table VII. The Mughabghab thermal total cross-section values were obtained by summing the capture, scattering, and paramagnetic cross sections. The RPI capture cross sections were calculated from the fitted param-

eters, and the total cross sections were taken directly from the transmission data. The double set of error bars for the capture cross sections represents the statistical accuracy of the transmission data (first error) and the estimated 10% uncertainty in the correction for paramagnetic scattering (second error). The uncertainty in the capture cross sections resulting from the uncertainties in the

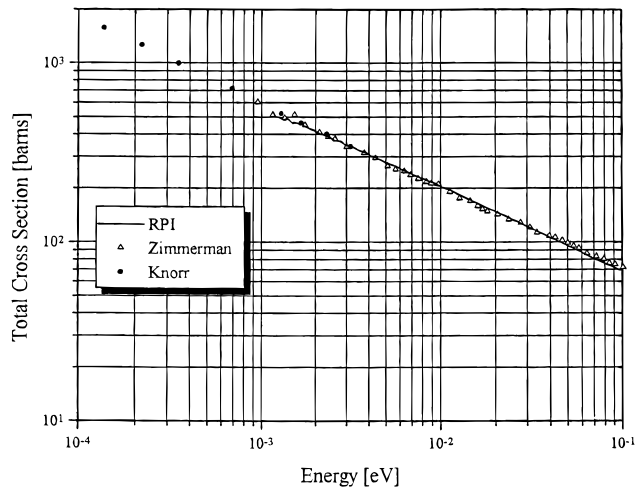


Fig. 7. Thulium thermal total cross section.

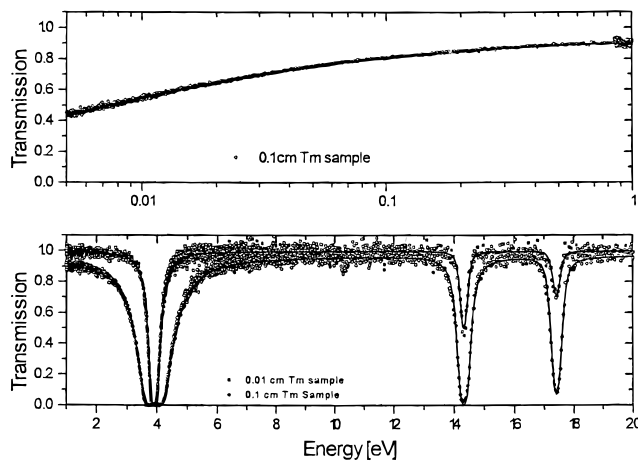


Fig. 8. Transmission data and SAMMY fit for the 0.01 and 0.1 cm thulium sample.

Mughabghab channel radii is  $<0.5$  b. The ENDF/B-VI capture and total cross sections were calculated from the resonance parameters. Note that the ENDF/B-VI total cross sections do not include paramagnetic scattering.

The total cross section of thulium is in good agreement with the values of Mughabghab and is well within the boundaries of the experimental errors. However, there is a significant difference in the capture cross section. As indicated in Ref. 5, this can be attributed to differences in the paramagnetic scattering used for correcting the transmission data before fitting the resonance parameters with SAMMY.

The RPI total cross section for erbium is  $\sim 2.5\%$  lower than the value quoted by Mughabghab. However, within the experimental errors, the values agree. This difference is also consistent with the observed difference in

TABLE VIII  
Thulium Resonance Parameters\*

Mughabghab			RPI		
$E$ (eV)	$\Gamma_\gamma$ (meV)	$\Gamma_n$ (meV)	$E$ (eV)	$\Gamma_\gamma$ (meV)	$\Gamma_n$ (meV)
-37	85	353.61	-37	85	257.4 (3.3)
-6	85	10.386	-6	85	19.25 (0.17)
3.91 (0.02)	96 (3)	8.133 (0.2)	3.9060 (0.0002)	102.4 (0.6)	7.380 (0.034)
14.50 (0.06)	84 (3)	9.2 (0.4)	14.324 (0.0006)	97.139 (1.187)	9.112 (0.063)
17.44 (0.03)	84 (4)	6.4 (0.8)	17.421 (0.0008)	81.356 (1.749)	5.69 (0.05)

\*Errors are in parentheses.

the capture cross sections of  $^{167}\text{Er}$ . Therefore, the RPI transmission data for the metallic and separated isotopes give a consistent set of data that is lower than the values quoted by Mughabghab and ENDF/B-VI. The  $^{167}\text{Er}$  capture cross section and its relatively large associated error quoted by Mughabghab still overlap the RPI value. For  $^{166}\text{Er}$ , another difference exists where the RPI data are lower by  $\sim 10\%$  compared to the value given by Mughabghab. The difference between these values is  $6.1 \pm 3.6$  b, where the error is the quadrature sum of errors from the two measurements. Thus, this difference is slightly more than one standard deviation and we conclude that the two measurements are effectively in agreement within statistics. The only other  $^{166}\text{Er}$  measurement by Vertebnyi et al.<sup>21</sup> gives a total cross section of  $48.75 \pm 2$  b (for more information, see Ref. 5, p. 142). This measurement is significantly lower than the other two, but is closer to the RPI value of  $53.8 \pm 0.6$  b than the value obtained from Mughabghab of  $59.9 \pm 3.6$  b.

The RPI total cross section for holmium is  $\sim 5\%$  higher than the value of Mughabghab. The RPI data are consistent with the measurement of Zimmerman et al. (see Sec. V.A). Observing the very good agreement in the capture cross section of holmium, it can be concluded that there is disagreement in the nuclear scattering or, as suggested before,<sup>5</sup> in the paramagnetic scattering cross section.

## VI. SUMMARY AND CONCLUSIONS

The ETT was used for a series of thermal transmission measurements of rare earth metallic samples of holmium, erbium, thulium, and enriched oxide samples of  $^{166}\text{Er}_2\text{O}_3$  and  $^{167}\text{Er}_2\text{O}_3$ . The measured total cross sections



of these isotopes in the energy range from 0.001 to 20 eV are presented and are in generally good agreement with other measurements but are in disagreement with ENDF/B-VI. The higher thermal flux of the ETT helped obtain data with small statistical errors. The thermal (0.0253 eV) total cross sections obtained from the data had smaller experimental errors relative to the values reported by Mughabghab. The two sets of errors listed for the RPI thermal capture cross sections reflect the accuracy of the total cross-section measurement (the first error) and the estimated 10% uncertainty in the nuclear and paramagnetic scattering subtraction (the second error). We recommend that the ENDF/B-VI total cross sections be reevaluated for these elements in the thermal energy region.

The total cross sections were corrected by subtracting the contributions from paramagnetic scattering. The data were then fitted with the SAMMY resonance analysis code. A sensitivity analysis shows that the radiation width of the lowest energy resonance is very sensitive to the thermal and subthermal cross section; therefore, the energy range of the resonance parameter fit was extended down to 0.002 eV.

New sets of resonance parameters were obtained by fitting several sample thicknesses and, in the case of erbium, also enriched oxide samples. The fits were also done over a wide energy range, from a few milli-electronvolts to 20 eV. Combining all these data sets resulted in a consistent set of parameters and good representation of the thermal region. These results can be further improved with a direct capture and, possibly, a scattering measurement. An accurate capture cross-section measurement coupled with this total cross-section measurement should lead to an accurate determination of nuclear and paramagnetic scattering in the thermal region.

#### REFERENCES

1. Y. DANON, R. E. SLOVACEK, and R. C. BLOCK, "The Enhanced Thermal Neutron Target at the RPI Linac," *Trans. Am. Nucl. Soc.*, **68**, 473 (1993).
2. Y. DANON, R. E. SLOVACEK, and R. C. BLOCK, "Design and Construction of a Thermal Neutron Target for the RPI Linac," *Nucl. Instrum. Methods A*, **352**, 396 (1995).
3. D. R. HARRIS, R. C. ROHR, D. K. HAYES, A. JONSSON, J. Y. JUNG, and R. Y. CHANG, "Critical Experiments and Analysis for ABB-CE Fuel with Erbium Burnable Absorber," *Trans. Am. Nucl. Soc.*, **65**, 414 (1992).
4. A. JONSSON, D. R. HARRIS, R. Y. CHANG, and O. J. THOMSEN, "Analysis of Critical Experiments with Erbium-Urania Fuel," *Trans. Am. Nucl. Soc.*, **65**, 415 (1992).
5. Y. DANON, "The RPI Enhanced Thermal Target and Total Cross Section Measurements of Ho, Tm and Er," PhD Thesis, Rensselaer Polytechnic Institute (1993).
6. D. B. SYME, "The Black and White-Filter Method for Background Determination in Neutron Time-of-Flight Spectrometry," *Nucl. Instrum. Methods*, **198**, 357 (1982).
7. G. T. TRAMMELL, "Magnetic Scattering of Neutrons from Rare Earth Ions," *Phys. Rev.*, **92**, 6 (1953).
8. M. BLUME, A. J. FREEMAN, and R.E. WATSON, "Neutron Magnetic Form Factors and X-Ray Atomic Scattering Factors for Rare Earth Ions," *J. Chem. Phys.*, **37**, 6 (1962).
9. Yu. A. ALEXANDROV, *Fundamental Properties of the Neutron*, Clarendon Press, Oxford (1992).
10. *Handbook of Chemistry and Physics*, Chemical Rubber Company, 73rd ed., CRC Press (1992).
11. M. C. MATTOS, "Paramagnetic Scattering of Neutrons by Rare-Earth Ions: Calculated Paramagnetic Scattering Cross Sections for Ce, Pr, Nd, Gd, Tb, Dy, Ho, Er, Tm, and Yb," *J. Chem. Phys.*, **48** (1968).
12. C. STASSIS, H. W. DECKMAN, B. N. HARMON, J. P. DESCLAUX, and A. J. FREEMAN, "Relativistic Magnetic Form Factors of Tripositive Rare-Earth Ions," *Phys. Rev. B*, **15**, 1, 369 (Jan. 1977).
13. N. LARSON, "Updated Users Guide for SAMMY: Multi-level R-Matrix Fits to Neutron Data Using Bayes Equation," ORNL/TM-9179/R2, Oak Ridge National Laboratory (1989).
14. "ENDF, Evaluated Nuclear Data Files," Brookhaven National Laboratory, National Nuclear Data Center, On-Line Data Service (1993).
15. S. F. MUGHABGHAB, M. DIVADEENAM, and N. E. HOLDEN, *Neutron Cross Sections*, Academic Press (1984).
16. G. I. BELL and S. GLASSTONE, *Nuclear Reactor Theory*, Robert E. Krieger Publishing Company, Malabar, Florida (1970).
17. R. L. ZIMMERMAN, L. Q. AMARAL, R. FULFARO, M. C. MATTOS, M. ABREU, and R. STASIULEVICIUS, "Neutron Cross Sections of Pr, Yb, Lu, Er, Ho and Tm," *J. Nucl. Phys. A*, **95**, 683 (1967).
18. SCHERMER, *Phys. Rev. B*, **136**, 1285 (1964).
19. K. KNORR and W. SCHMATZ, "Total Cross Sections of the Elements Tb, Dy, Ho, Er, Tm and Lu for Subthermal Neutrons," *Atomkernenergie/Kerntechnik*, **16**, 9, 49 (1970).
20. J. R. ROESSER and R. E. SLOVACEK, "Erbium and Pyrolytic Graphite Slow Neutron Cross Sections," *Trans. Am. Nucl. Soc.*, **3**, 2, 462 (1960).
21. V.P. VERTEBNYI, M. F. VLASOV, V. V. KOLOTYI, A. L. KIRLIJUKM, V. PASECHNIK, T. I. PISANKO, N. L. GNIDAK, and A. I. KAL'CHENKO, "Neutron Cross Section of Erbium Isotopes in the Energy Range 0.007-200 eV," *Proc. Int. Conf. Study of Nuclear Structure with Neutrons*, Antwerp, Belgium, 1965, p. 186.